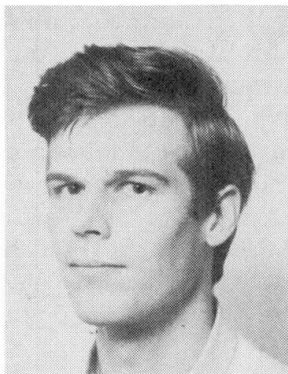# Stability and Uniqueness in Numerical Modelling of Concrete Structures
Stabilité et unicité des modèles numériques dans les structures en béton
Stabilität und Eindeutigkeit numerischer Modelle im Stahlbeton

René de BORST
TNO-IBBC
Delft, The Netherlands

René de Borst, born 1958, earned his Ir. degree in civil engineering in 1982 and his Dr. degree in 1986, both from Delft University of Technology. He has been a member of the DIANA group of the TNO Institute for Building Materials and Structures since 1982.

SUMMARY

Recent advances in smeared crack modeling and computational techniques for concrete structures are reviewed. Special attention is given to the issue of stability and uniqueness in numerical computations of strain-softening concrete. Techniques for overcoming bifurcation and limit points are discussed whereby special attention is given to cases with highly localized failure modes. The techniques are applied to some reinforced and unreinforced concrete structures.

RÉSUMÉ

Les progrès récents dans la modélisation des fissures homogénéisées et les techniques de calcul à l'ordinateur pour les structures en béton sont passés en revue. Une attention particulière est portée au cas de la stabilité et de l'unicité, dans de nombreux calculs, du béton se plastifiant sous contrainte. Des techniques pour résoudre les problèmes de bifurcation et de points limites sont discutées et une attention particulière est portée aux cas de modes de rupture hautement localisés. Les techniques sont appliquées à certaines structures en béton armé et non-armé.

ZUSAMMENFASSUNG

In diesem Beitrag wird eine Übersicht über neue Entwicklungen der ausgeglichenen Rissbildung und Rechenverfahren für Betonkonstruktionen gegeben. Hauptaugenmerk wird gerichtet auf Stabilität und Eindeutigkeit in numerischen Berechnungen von entfestigendem Beton. Lösungsmethoden zur Vermeidung von Bifurkation und Grenzwerte werden diskutiert für höchstbelastete Bereiche. Die Methoden werden auf einige bewehrte und unbewehrte Betonkonstruktionen angewandt.

1. INTRODUCTION

Concrete is a very complicated material because of its heterogeneity, the presence of reinforcement, the low tensile strength, the change in properties when it matures, and so on. It is therefore not surprising that predictions of the mechanical behavior of concrete structures still suffer from a lack of reliability. Nevertheless, the discrepancy between analytical results and the real behavior is often greater than necessary when considering the current level of sophistication of testing procedures, constitutive models and computational techniques. Significant, and in some areas seemingly insurmountable difficulties persist, but progress has definitely been made in analyzing concrete structures with aid of finite elements.

It is the purpose of the present paper to give an overview of some recent achievements of the DIANA-group in constitutive modeling and the application of computational techniques to concrete structures. The review is by no means intended to be exhaustive, and important issues like for instance time-dependent behavior [11,13] or bond-slip behavior [27] will not be treated. The main topics which will be considered, are smeared crack modeling and issues regarding stability and uniqueness of computations for concrete structures. It is recognized that the crack model, which we will henceforth refer to as the DIANA-crack model, has been treated extensively in previous publications [7,8,10,13,26,29], but because crack formation plays such a pivotal role in the behavior of concrete structures, there may be some justification in briefly reviewing the main concepts of it before discussing issues regarding stability and uniqueness.

2. MODELING OF SMEARED CRACKING

The fundamental feature of the employed smeared crack model is a decomposition of the total strain rate into a concrete strain rate $\dot{\varepsilon}^{co}$ and into a crack strain rate $\dot{\varepsilon}^{cr}$ (e.g., also [4,22]):

$$\dot{\varepsilon} = \dot{\varepsilon}^{co} + \dot{\varepsilon}^{cr} \tag{1}$$

The concrete strain rate itself may also be composed of several contributions e.g., an elastic part and a viscous part. Similarly, the crack strain rate $\dot{\varepsilon}^{cr}$ may be decomposed into several contributions:

$$\dot{\varepsilon}^{cr} = \dot{\varepsilon}_1^{cr} + \dot{\varepsilon}_2^{cr} + \ldots\ldots\ldots \tag{2}$$

where $\dot{\varepsilon}_1^{cr}$ is the strain rate of a primary crack, $\dot{\varepsilon}_2^{cr}$ is the strain rate of a secondary crack and so on. Combining eqs. (1) and (2), we obtain

$$\dot{\varepsilon} = \dot{\varepsilon}^{co} + \dot{\varepsilon}_1^{cr} + \dot{\varepsilon}_2^{cr} + \ldots\ldots\ldots \tag{3}$$

The relation between the strain rate of a particular crack (either primary or secondary) and the stress rate is most conveniently defined in the coordinate system which is aligned with the crack. This necessitates a transformation between the crack strain rate $\dot{\varepsilon}_n^{cr}$ of crack n in the global x,y,z-coordinates and a crack strain rate $\dot{e}_n^{cr}$ which is expressed in local coordinates. Restricting the treatment to a two-dimensional configuration (which is not essential), we observe that a crack only has a normal strain rate $\dot{e}_n^{cr}$ and a shear strain rate $\dot{\gamma}_n^{cr}$, so that

$$\dot{e}_n^{cr} = (\dot{e}_n^{cr} \quad \dot{\gamma}_n^{cr})^T \tag{4}$$

where the superscript T denotes a transpose. The relation between $\dot{\varepsilon}_n^{cr}$ and $\dot{e}_n^{cr}$ reads

$$\dot{\varepsilon}_n^{cr} = N_n \dot{e}_n^{cr} \tag{5}$$

with

$$N_n = \begin{bmatrix} \cos^2\vartheta_n & -\sin\vartheta_n\cos\vartheta_n \\ \sin^2\vartheta_n & \sin\vartheta_n\cos\vartheta_n \\ 2\sin\vartheta_n\cos\vartheta_n & \cos^2\vartheta_n - \sin^2\vartheta_n \end{bmatrix} \tag{6}$$

where ϑ_n is the inclination angle of the normal of crack n with the x-axis. Substitution of eq. (5) in eq. (2) gives for multiple cracks

$$\dot{\varepsilon}^{cr} = N_1 \dot{e}_1^{cr} + N_2 \dot{e}_2^{cr} + \ldots\ldots\ldots\ldots \tag{7}$$

For the derivation of the stress-strain law of the system of cracks and concrete, it is convenient to assemble all the crack strain rates which are expressed in their own local coordinate system in a vector $\dot{e}^{cr}$,

$$\dot{e}^{cr} = (\dot{e}_1^{cr} \quad \dot{\gamma}_1^{cr} \quad \dot{e}_2^{cr} \quad \dot{\gamma}_2^{cr} \ldots\ldots\ldots\ldots)^T \tag{8}$$

When we also introduce the matrix N,

$$N = [N_1 \ N_2 \ \ldots\ldots\ldots\ldots] \tag{9}$$

we observe that we can rewrite eq. (7) as

$$\dot{\varepsilon}^{cr} = N\dot{e}^{cr} \tag{10}$$

In a similar way, we can define a vector $\dot{s}_n$

$$\dot{s}_n = (\dot{s}_1 \quad \dot{t}_1)^T \tag{11}$$

with $\dot{s}_n$ the normal and $\dot{t}_n$ the shear stress rate in crack n of the integration point. The vector $\dot{s}$ which assembles all stress rates with respect to their own local coordinate system then reads:

$$\dot{s} = (\dot{s}_1 \quad \dot{t}_1 \quad \dot{s}_2 \quad \dot{t}_2 \ldots\ldots\ldots\ldots\ldots)^T \tag{12}$$

and the relation between the stress rate in the global coordinate system $\dot{\sigma}$ and the stress vector $\dot{s}$ can be derived to be

$$\dot{s} = N^T \dot{\sigma} \tag{13}$$

To complete the system of equations, we need a constitutive model for the intact concrete and a stress-strain relation for the smeared cracks. For the concrete between the cracks we assume a relationship which has the following structure

$$\dot{\sigma} = D^{co} \dot{\varepsilon}^{co} \tag{14}$$

where the matrix D^{co} contains the instantaneous moduli of the concrete. The formalism of eq. (14) can be extended to deal with phenomena like thermal dilatation, shrinkage and creep [11,13], but this will not be pursued in the present paper. In a similar way, we can define a relation between the crack strain rate $\dot{e}_n^{cr}$ of crack n and the stress rate $\dot{s}_n$ in that crack. In this paper, we will assume a relation which formally reads:

$$\dot{s}_n = D_n^{cr} \dot{e}_n^{cr} \tag{15}$$

with D_n^{cr} a 2*2 matrix. For the derivation of the stress-strain relation of the cracked concrete, it is again convenient to assemble all the matrices D_n^{cr} in a matrix D^{cr},

$$D^{cr} = \begin{bmatrix} D_1^{cr} & 0 & \ldots \\ 0 & D_2^{cr} & \ldots \\ \ldots & \ldots & \ldots \end{bmatrix} \tag{16}$$

so that the relation between $\dot{s}$ and $\dot{e}^{cr}$ reads

$$\dot{s} = D^{cr} \dot{e}^{cr} \tag{17}$$

Using eqs. (1), (10), (13), (14) and (17) we can obtain the compliance relation for the cracked concrete:

$$\dot{\varepsilon} = \left\{ C^{co} + NC^{cr} N^T \right\} \dot{\sigma} \tag{18}$$

with $C^{co} = (D^{co})^{-1}$ and $C^{cr} = (D^{cr})^{-1}$ the compliance matrices of the concrete and the cracks respectively. With aid of the Sherman-Morrison-Woodbury formula we can also obtain the

stiffness relation

$$\dot{\sigma}=\left\{D^{co}-D^{co}\,N\,[\,D^{cr}+N^T D^{co}\,N\,]^{-1}N^T D^{co}\right\}\dot{\varepsilon}$$

(19)

The success of this multiple crack model is contingent upon a proper formulation of the constitutive matrix

$$D_n^{cr}=\begin{bmatrix}D_{11}^{cr} & D_{12}^{cr}\\ D_{21}^{cr} & D_{22}^{cr}\end{bmatrix}$$

(20)

for the smeared-out cracks. Fortunately, in many concrete structures the crack strains are so small that coupling effects between the normal crack strain and the shear stress, or between the shear crack strain and the normal stress can be disregarded, so that we may set the off-diagonal terms in eq. (20) equal to zero ($D_{12}^{cr}=0$ and $D_{21}^{cr}=0$). If, such as in crack-dilatancy models [4,32] or in jointed rock masses [2], D_{12}^{cr} and D_{21}^{cr} can not be assumed to vanish, we face significant additional difficulties, since the values for D_{12}^{cr} and D_{21}^{cr} generally differ considerably. This implies that D_n^{cr} becomes nonsymmetric, which also destroys the major symmetry of eq. (19). Apart from the fact, that this leads to significantly larger CPU-times, it also has consequences for the stability of the model, as will be briefly discussed in the sequel of this paper.

The tangent modulus D_{11}^{cr} represents the relation between the normal crack strain rate and the normal stress rate. In practice, D_{11}^{cr} is negative as we normally have a descending relation between $\dot{s}_n$ and $\dot{e}_n^{cr}$. However, the evaluation of D_{11}^{cr} from test data entails a complication, as recent research [5,21] indicates that a straightforward translation from experimental data in a value for D_{11}^{cr} leads to results which are not objective with regard to mesh refinement. To overcome this problem, it has been proposed to consider the fracture energy G_f [5,21] as the fundamental parameter which governs crack propagation. It is beginning to emerge gradually that this so-called "tension-softening" model is not free from deficiencies. This is particularly so when we allow for the possibility of multiple cracks. Suppose that a primary crack has been created with a D_{11}^{cr} determined from the fracture energy G_f. If upon formation of a secondary crack the same crack stress-strain relation is adopted for the second crack, the fracture energy will be consumed twice. If both cracks are orthogonal to each other, this is not unrealistic, but for any other inclination angle it seems incorrect. Hence, the concept of a fracture energy as outlined above does not seem to suffice for multiple crack formation. Indeed, a solution in which the fracture energy is distributed over both cracks is not correct as the fracture energy G_f is not a scalar, but a vector although this does not seem to have been recognized widely.

The shear modulus D_{22}^{cr} of the crack is usually assigned a constant value. This leads to the anomaly that for very large crack strains we continue to compute an increase of the shear stresses transferred across a crack, which may result in shear stresses of more than 15 N/mm^2. A shear-softening model, quite similar to the tension-softening model, has recently been proposed to remedy this anomaly [29]. Deployment of this model resulted in a major improvement for some unreinforced shear beams, especially in the post-peak regime.

It is finally noted that the structure of eq. (19) is quite similar to the structure of an elastoplastic stiffness tensor at a yield vertex. Indeed, any constitutive law in which a decomposition in the sense of eq. (1) is assumed, will lead to an equation with a similar structure. This holds true for a yield vertex in which two yield surfaces are active, but for instance also for the intersection of a yield surface and a fracture surface [13,14].

3. STABILITY AND UNIQUENESS OF DISCRETE MECHANICAL SYSTEMS

A body is said to be in a state of stable equilibrium if the response on a vanishingly small disturbance also remains vanishingly small [20]. This condition is usually replaced by the condition that

$$U=\int_V \dot{\boldsymbol{\varepsilon}}^T \dot{\boldsymbol{\sigma}}\, dV \tag{21}$$

is positive for all kinematically admissible strain rate fields $\dot{\boldsymbol{\varepsilon}}$, while the equilibrium is unstable under dead loading if U becomes negative for at least one kinematically admissible strain rate field. Although it has not been proved rigorously for all classes of constitutive models that the criterion that the second-order work (eq. 21) is positive, is indeed equivalent to the abovementioned definition, it seems to be a reasonable hypothesis.

For an incrementally-linear constitutive model,

$$\dot{\boldsymbol{\sigma}}=\boldsymbol{D}\dot{\boldsymbol{\varepsilon}} \tag{22}$$

with $\boldsymbol{D}$ the matrix which contains the stiffness moduli, eq. (21) can be replaced by

$$U=\int_V \dot{\boldsymbol{\varepsilon}}^T \boldsymbol{D}\dot{\boldsymbol{\varepsilon}}\, dV \tag{23}$$

Since we have, for the skew-symmetric part of $\boldsymbol{D}$, $\dot{\boldsymbol{\varepsilon}}^T[\boldsymbol{D}-\boldsymbol{D}^T]\dot{\boldsymbol{\varepsilon}}=0$, we can write eq. (23) also as

$$U=\tfrac{1}{2}\int_V \dot{\boldsymbol{\varepsilon}}^T[\boldsymbol{D}+\boldsymbol{D}^T]\dot{\boldsymbol{\varepsilon}}\, dV \tag{24}$$

Consequently, stability under dead loading is no longer assured if

$$\int_V \dot{\boldsymbol{\varepsilon}}^T[\boldsymbol{D}+\boldsymbol{D}^T]\dot{\boldsymbol{\varepsilon}}\, dV=0 \tag{25}$$

for at least one kinematically admissible $\dot{\boldsymbol{\varepsilon}}$.

To investigate the implications of the stability requirement $U>0$ for discrete mechanical systems such as arise in finite element applications, we divide the continuum in an arbitrary number of finite elements, and we interpolate the continuous velocity field $\boldsymbol{v}$ as follows:

$$\boldsymbol{v}=\boldsymbol{H}\dot{\boldsymbol{a}} \tag{26}$$

in which the matrix $\boldsymbol{H}$ contains the interpolation polynomials and $\boldsymbol{a}$ is a vector which contains the nodal displacements (e.g., [3]). The relation between the velocity field $\boldsymbol{v}$ and the strain rate $\dot{\boldsymbol{\varepsilon}}$ can formally be written as

$$\dot{\boldsymbol{\varepsilon}}=\boldsymbol{L}\boldsymbol{v} \tag{27}$$

with $\boldsymbol{L}$ a matrix which contains differential operators. The relation between the nodal velocities and the strain rate then becomes

$$\dot{\boldsymbol{\varepsilon}}=\boldsymbol{B}\dot{\boldsymbol{a}} \tag{28}$$

where the notation $\boldsymbol{B}=\boldsymbol{L}\boldsymbol{H}$ has been introduced.

With the notations and the definitions of the preceding, we can rewrite the stability condition (23) as

$$\int_V \dot{\boldsymbol{a}}^T \boldsymbol{B}^T \boldsymbol{D}\boldsymbol{B}\dot{\boldsymbol{a}}\, dV>0 \tag{29}$$

for all kinematically admissible velocity fields $\dot{\boldsymbol{a}}$. With the notation

$$\boldsymbol{K}=\int_V \boldsymbol{B}^T \boldsymbol{D}\boldsymbol{B}\,dV \tag{30}$$

for the tangent stiffness matrix of the underlying system, we obtain that the stability of the equilibrium of a discrete mechanical system becomes critical if

$$\dot{\boldsymbol{a}}^T \boldsymbol{K}\dot{\boldsymbol{a}}=0 \tag{31}$$

for at least one kinematically admissible vector $\dot{\boldsymbol{a}}$. This condition is satisfied if

$$\det(\boldsymbol{K})=0 \tag{32}$$

which according to Vieta's rule,

$$\det(K) = \prod_{i=1}^{n} \lambda_i \qquad (33)$$

with λ_i the eigenvalues of K, implies that at least one eigenvalue vanishes. For symmetric systems, eq. (32) is not only a sufficient, but also a necessary condition for eq. (31) to hold. However, for nonsymmetric matrices K eq. (31) may also be satisfied when $\dot{a}$ is orthogonal to $K\dot{a}$. Hence, the vanishing of $\det(K)$ or alternatively, the vanishing of at least one eigenvalue of K implies that the equilibrium is in a critical state, but for nonsymmetric systems this critical state can also be attained when all eigenvalues of the tangent stiffness matrix of the underlying solid are non-zero. Put differently, *the positiveness of the eigenvalues of K is a necessary, but not a sufficient condition for stability of a mechanical system which is governed by a nonsymmetric matrix K.*

Let us next consider eq. (25), i.e., the case that we have removed the skew-symmetric part from the functional of eq. (23). Then, we obtain that the equilibrium of a discrete mechanical system becomes neutrally stable if

$$\dot{a}^T\left[K+K^T\right]\dot{a}=0 \qquad (34)$$

for at least one kinematically admissible velocity field. Since $K+K^T$ is symmetric, this condition is satisfied if and only if

$$\det(K+K^T)=0 \qquad (35)$$

or equivalently, U vanishes if and only if an eigenvalue of $K+K^T$ vanishes. Consequently, *the positiveness of the eigenvalues of the matrix $K+K^T$ is a sufficient and necessary condition for the stability of a discrete mechanical system which is governed by a nonsymmetric tangent stiffness matrix K.* For the limiting case of a symmetric stiffness matrix we recover the classical notion that we have stability when all eigenvalues of the tangent stiffness matrix K of the underlying solid are positive.

With regard to uniqueness of solution, we observe that incremental equilibrium must be complied with at each instant in the loading process

$$\int_V B^T \dot{\sigma}dV=\mu q^* \qquad (36)$$

In it, μ is the loading rate, and q^* is a normalized load vector. Suppose that there would be another stress rate distribution, which would result from the loading rate μ and which would also satisfy incremental equilibrium. The *difference* $\Delta\dot{\sigma}$ of both stress rate distributions would then satisfy the condition that

$$\int_V B^T \Delta\dot{\sigma}dV=0 \qquad (37)$$

With eqs. (22), (28) and (30), we can rewrite eq. (37) as

$$K\Delta\dot{a}=0 \qquad (38)$$

with $\Delta\dot{a}$ the difference between both velocity fields. A non-trivial solution may then exists if and only if

$$\det(K)=0 \qquad (39)$$

or equivalently, if at least one eigenvalue of K vanishes. If a non-trivial solution indeed exists, such a point is commonly named a bifurcation point. Several equilibrium branches emanate from such a point. There is yet another possibility that $\det(K)$ vanishes. If the load reaches a maximum, μ vanishes, and eq. (36) reduces to

$$K\dot{a}=0 \qquad (40)$$

so that for a non-zero vector $\dot{a}$ we also find that eq. (39) must be fulfilled. The latter possibility is called a limit point.

In passing from eq. (37) to eq. (38) it has been tacitly assumed that both strain rates are related to stress rates by the same matrix of (tangential) moduli D. For elastic-plastic or elastic-fracturing solids, where we have different behavior in loading and unloading, this is not necessary. Strictly speaking, we have to investigate all possible combinations of loading and unloading for such a multi-valued constitutive law in order to determine whether eq. (37) holds true for some $\Delta\dot{a}$.

For nonsymmetric stress-strain laws, the situation is even more complicated, since $\det(K+K^T)$ may vanish prior to the vanishing of $\det(K)$. Hence, loss of stability may precede loss of uniqueness of solution for solids with a nonsymmetric stress-strain relation.

Although there seems no convenient procedure available to determine whether a solution is unique or not, the presence of negative eigenvalues of the tangent stiffness matrix K conversely clearly indicates the existence of alternative equilibrium branches or the fact that we have passed a limit point. In the case that we have passed a limit point, which implies that the load is descending, we find one negative eigenvalue which is associated with the descending branch. The other possibility is that the negative eigenvalues belong to alternative equilibrium states so that we have passed a bifurcation point. Again, two possibilities arise, since the basic path after bifurcation may be ascending or descending. If it is still ascending, all the, say m negative eigenvalues can be associated with m alternative equilibrium states which can in principle be reached via a suitable combination of the incremental displacement vector of the basic path and the corresponding eigenvector, as detailed in the next section. If the basic path is descending after passing a bifurcation point, one negative eigenvalue is associated with the descending basic path, while the remaining negative eigenvalues correspond to $m-1$ alternative equilibrium states.

A final remark addresses the question whether the alternative equilibrium states are indeed accessible. If a mechanical system is undergoing a continuous process, such an alternative equilibrium state can only be reached via an equilibrium path. If a bifurcation point has been passed and the system is on a path of unstable equilibrium thereafter, it will continue on this unstable path because other equilibrium states cannot be reached under dead loading conditions. If a *temporal* discretization of the loading process is employed, i.e. if the loading program is subdivided into a number of finite intervals, alternative equilibrium states can also be reached via non-equilibrium paths, because we then essentially deal with equilibrium states and not with equilibrium paths. In fact, we obtain a sequence of non-equilibrium states when iterating to a converged solution. An example of reaching a new equilibrium state via a number of non-converged states will be given at the end of this paper.

4. NUMERICAL APPROACH FOR POST-BIFURCATION AND POST-FAILURE BEHAVIOR

In numerical applications, the lowest eigenvalue will never become exactly zero because of round-off errors. Rather, we monitor the sign of the eigenvalues of the tangent stiffness matrix and when we encounter a negative eigenvalue while the load is rising, or when we compute more than one negative eigenvalue while the load is descending, we conclude that we have passed a bifurcation point.

Continuation on an alternative equilibrium branch can then be forced by adding a part of the eigenmode v_1, which belongs to the vanishing eigenvalue, to the incremental displacement field of the fundamental path Δa^* [8,12,24]

$$\Delta a = \Delta a^* + \beta v_1 \tag{41}$$

with β a scalar. The magnitude of β is fixed by second-order terms or by switch conditions for elastoplasticity or for plastic-fracturing materials. The most simple way to determine β numerically is to construct a trial displacement increment Δa such that it is orthogonal to the basic path:

$$\Delta a^T \Delta a^* = 0 \tag{42}$$

Substituting eq. (41) in this expression yields for Δa

$$\Delta a = \Delta a^* - \frac{(\Delta a^*)^T \Delta a^*}{(\Delta a^*)^T v_1} v_1 \tag{43}$$

Eq. (43) fails when $(\Delta a^*)^T v_1 = 0$, i.e., when the eigenmode is orthogonal to the basic path. A simple remedy is to normalize Δa such that [8,12],

$$(\Delta a^*)^T \Delta a^* = \Delta a^T \Delta a \tag{44}$$

or to put

$$\Delta a^* = \sqrt{\Delta a^T \Delta a}\, v_1 \tag{45}$$

in such cases.

In general, the bifurcation path will not be orthogonal to the fundamental path, but when we add equilibrium iterations, the orthogonality condition (42) will maximize the possibility that we converge to a bifurcation branch and not to the basic path, although this is not necessarily the lowest bifurcation path when there emanate several equilibrium branches from the bifurcation point. When we do not converge on the lowest bifurcation path, this will be revealed by negative eigenvalues of the stiffness matrix of the bifurcated solution. The above described procedure can then be repeated until we ultimately arrive at the lowest bifurcation path.

The procedure described in the preceding is well suited for assessing post-bifurcation behavior. Bifurcations however are rather rare in normal structures owing to imperfections, and even if a bifurcation point exists, numerical round-off errors and spatial discretization usually transfer the bifurcation point into a limit point unless we have a homogeneous stress field.This observation does not render the approach to bifurcation problems worthless as it provides a thorough insight which is of importance for the associated limit problems, but it is obvious that numerical procedures must also be capable of locating limit points and tracing post-limit behavior.

In a nonlinear finite element analysis, the load is applied in a number of small increments (e.g., [3]). Within each load increment, equilibrium iterations are applied and the iterative improvement δa_i in iteration number i to the displacement increment Δa_{i-1} is given by

$$\delta a_i = K_{i-1}^{-1}\left[p_{i-1} + \Delta\mu_i q^*\right] \tag{46}$$

K_{i-1} is the possibly updated stiffness matrix, $\Delta\mu_i$ is the value of the load increment which may change from iteration to iteration and p_{i-1} is defined by

$$p_{i-1} = \mu_0 q^* - \int_V B^T \sigma_{i-1} dV \tag{47}$$

In (47), the symbols μ_0 and σ_{i-1} have been introduced for the value of the scalar load parameter at the beginning of the current increment and the stress vector at iteration number $i-1$.

The essence of controlling the iterative solution procedure indirectly by displacements, is that δa_i is conceived to be composed of two contributions

$$\delta a_i = \delta a_i^I + \Delta\mu_i\, \delta a_i^{II} \tag{48}$$

with

$$\delta a_i^I = K_{i-1}^{-1} p_{i-1} \tag{49}$$

and

$$\delta a_i^{II} = K_{i-1}^{-1} q^* \tag{50}$$

After calculating the displacement vectors δa_i^I and δa_i^{II}, $\Delta\mu_i$ is determined from some constraint equation on the displacement increments and Δa_i is subsequently calculated from

$$\Delta a_i = \Delta a_{i-1} + \delta a_i \tag{51}$$

Crisfield [15] for instance uses the norm of the incremental displacements as constraint

equation

$$\Delta a_i^T \Delta a_i = \Delta l^2 \tag{52}$$

where Δl is the arc-length of the equilibrium path in the n-dimensional displacement space. The drawback of this so-called spherical arc-length method is that it yields a quadratic equation for the load increment. To circumvent this problem, we may linearize eq. (52), yielding [23]:

$$\Delta a_i^T \Delta a_{i-1} = \Delta l^2 \tag{53}$$

This method, known as the updated normal path method, results in a linear equation for the load increment. With the additional approximation [8,12]

$$\delta a_i \approx 2(\Delta a_i - \Delta a_{i-2}) \tag{54}$$

we obtain for $\Delta \mu_i$:

$$\Delta \mu_i = -\frac{\Delta a_{i-1}^T \delta a_i^I}{\Delta a_{i-1}^T \delta a_i^{II}} \tag{55}$$

Both eqs. (52) and (53) have been employed successfully within the realm of geometrically nonlinear problems, where snapping and buckling of thin shells can be traced quite elegantly. Nevertheless, for materially nonlinear problems the method sometimes fails, which may be explained by considering that for materially nonlinear problems, failure or bifurcation modes are often highly localized. Hence, *only a few nodes contribute to the norm of displacement increments, and failure is not sensed accurately by such a global norm*. As straightforward application of eqs. (52) or (53) is not always successful, we may amend these constraint equations by applying weights to the different degrees of freedom or omitting some of them from the constraint equation. The constraint equation (53) then changes into

$$\Delta u_i^T \Delta u_{i-1} = \Delta l^2 \tag{56}$$

where Δu_i contains only a limited number of the degrees of freedom of those of Δa_i, and eq. (55) changes in a similar fashion. The term "arc-length" control now no longer seems very appropriate, and the term "indirect displacement control" is probably more suitable. The disadvantage of modifying the constraint equation is that the constraint equation becomes problem dependent. As a consequence, the method loses some of its generality and elegance.

5. EXAMPLES

We will now illustrate some of the procedures discussed in the preceding by a few examples and we will begin with the simple case of an unreinforced bar loaded in pure tension. This example has been used before by other researchers [16], but so much insight can be gained from it, both in a theoretical and in a numerical sense, that we will again resort to it. The bar is modeled with m elements and is composed of an elastic-softening material with an ultimate strain ε_u at which the tensile strength has vanished completely. ε_u is assumed to be equal to n times the strain at the tensile strength. A perfect bar would deform uniformly throughout the loading process and the load-deflection curve is simply a copy of the imposed stress-strain law. However, if one element has a slight imperfection, only this element will show loading while the other elements will show unloading. Then, the imposed stress-strain law at a local level is not reproduced. Instead, an average strain is calculated in the post-peak regime which is smaller than the strain of the stress-strain law since the element which shows loading, will follow the path A-B in Fig. 1, while the other elements will follow the path A-C. This implies that when all elements have the same dimensions, we have for the average strain increment $\Delta \bar{\varepsilon}$

$$\Delta \bar{\varepsilon} = \left[\frac{n}{m} - 1\right] \frac{\Delta \sigma}{E} \tag{57}$$

Consequently, when we increase the number of elements while keeping the length of the bar fixed, the average strain in the post-peak regime gradually becomes smaller and for $m > n$ the
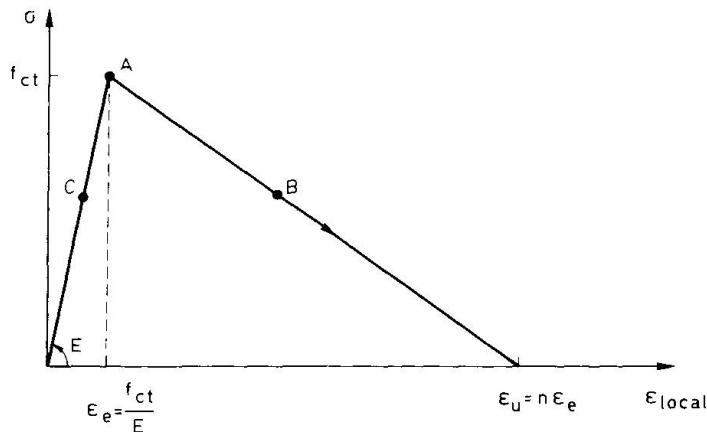
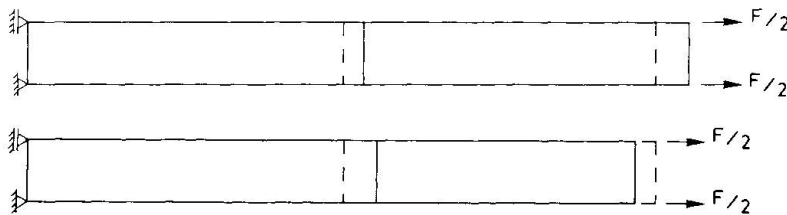**Fig. 1.** Stress vs. average strain for an unreinforced bar.

Fig. 2. Eigenmodes for two-element bar just beyond the limit point.
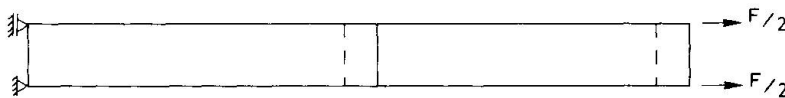

Fig. 3. Total displacements at zero load level.

average strain in the post-peak regime even becomes *smaller* than the strain at peak load. This implies that for $m > n$, the load-deflection curve shows a *snap-back* [8,12,17,29,30]. Obviously, *"snap-back"* behavior cannot be analyzed under direct displacement control, but only with indirect displacement control. Yet, the possibility of this phenomenon has been ignored frequently in the past, and many analyses have been terminated at such a point because of divergence of the iterative procedure. A further parallel can be drawn with experiments which can not be carried out properly under displacement control, e.g., with shear or other brittle failures. The observed explosive failure is then simply the result of an attempt to traverse an equilibrium path under improper static loading conditions.

A numerical simulation of this problem is shown in Figs. 2 and 3 for the case that the bar is divided in two elements and that the length of the softening branch is equal to ten times the strain at the tensile strength ($m = 2$ and $n = 10$). In this case a perfect bar is loaded just beyond the limit load, using indirect displacement control (eq. 56). If the solution is continued the solid post-peak line of Fig. 1 is obtained. However, when we carry out an eigenvalue analysis of the tangent stiffness matrix just beyond peak strength (Fig. 2) and perturb the fundamental solution using eq. (41), we obtain the localization of Fig. 3. Continuing the solution then results in an ultimate average strain $\bar{\varepsilon} = \frac{1}{2} \varepsilon_u$.

From the preceding discussion it will be clear that the response of an imperfect bar in the post-failure regime will depend upon the number of elements and the degree of interpolation within the elements. It has been attempted to control this mesh-dependence in the softening regime using energy approaches [5,25,26,28,33]. Such approaches can only be partially successful since the spread of the softening region is not known in advance. Consequently, the observation that use of a local softening law may involve snap-back behavior on structural level and to a strongly mesh-dependent and a non-unique post-peak response may hold even when such an energy approach is adopted. This is exemplified by the beam of Figs. 4 and 5, which exhibits a violent snap-back behavior in spite of the fact that the length of the softening branch had been adapted to some structural size. Also, the mesh-dependence of the calculated failure
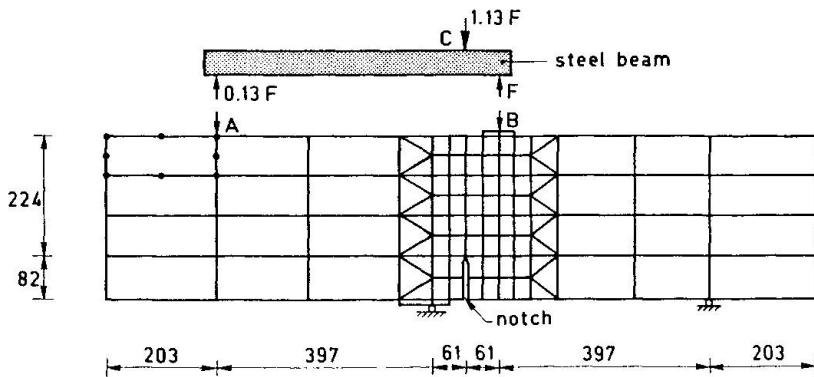
Fig. 4. Element mesh and dimension for unreinforced beam [1].
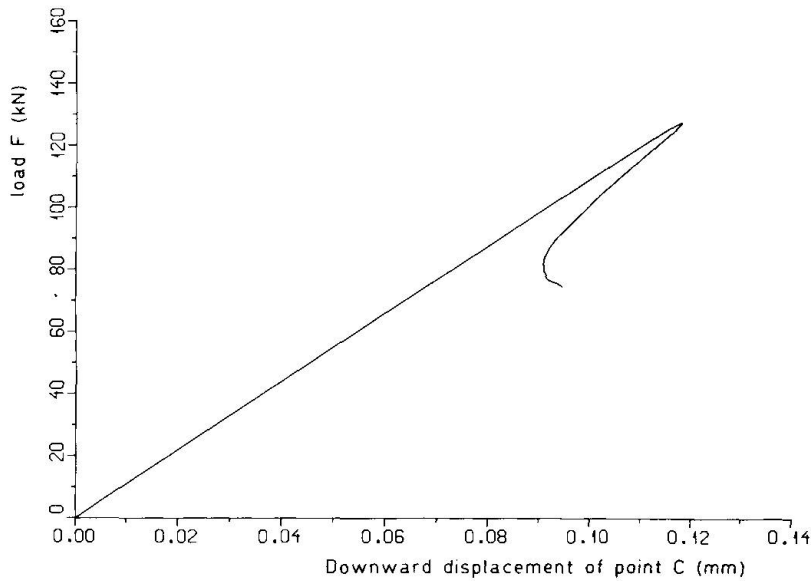
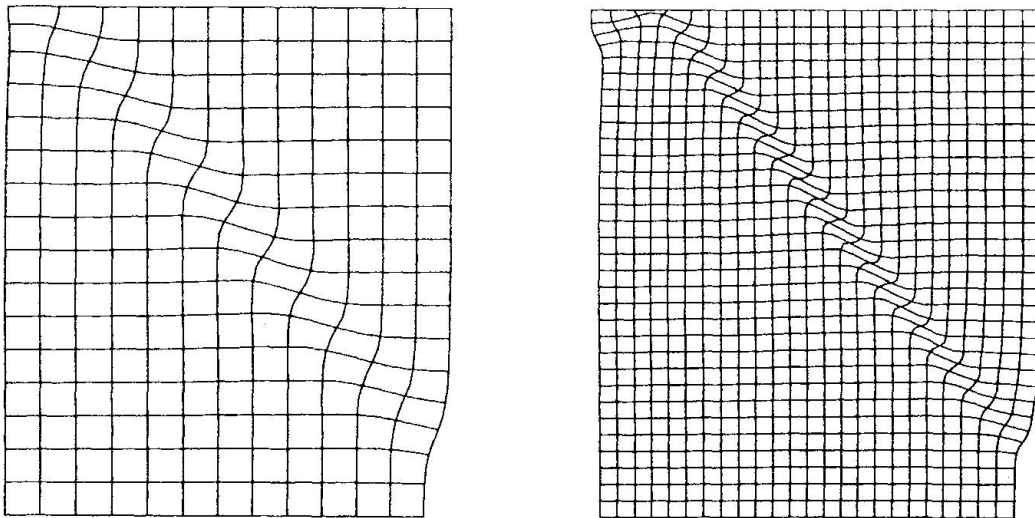

Fig. 5. Load-deflection curve for point C.

Fig. 6. Incremental displacements for a biaxial test on a sand sample. The failure state shows a strong mesh-dependence.

mode persists. This is demonstrated by the example of Fig. 6, which is a bifurcation analysis for a (plane-strain) biaxal test on sand. We observe that the width of the shear band which develops, is highly dependent on the fineness of the grid [8,9]. A possible solution to these basic deficiencies might be the use of non-local constitutive laws in the softening regime [6,31].
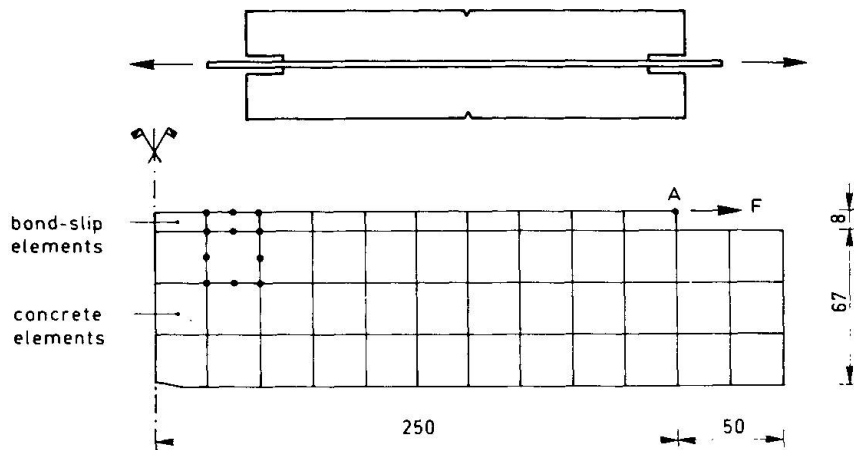
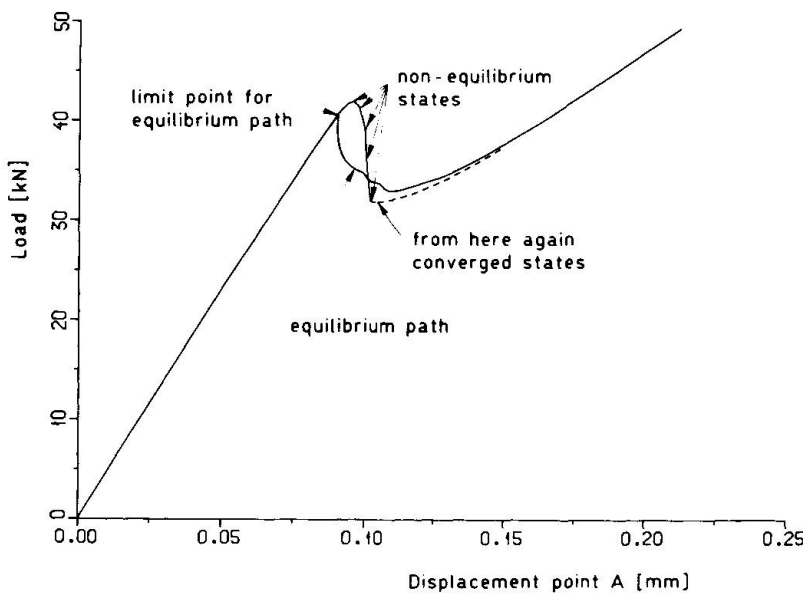**Fig. 7.** Element mesh and dimensions for tension-pull specimen [19].

Fig. 8. Load-deflection curve for point A.

Addition of reinforcement not always improves the behavior described in the preceding. When the reinforcement is densely distributed, we mostly obtain a rather ductile response and we seldom encounter numerical difficulties, but when we have a dominant, concentrated reinforcing bar, the presence of reinforcement only adds to the possibility that spurious alternative equilibrium states and snap-back behavior occur [12,17]. We will demonstrate this by the simple tension-pull specimen of Fig. 7 [19]. The reinforcing bar is given by the line AB and a linear bond-slip law is assumed between the concrete and the reinforcement. For the concrete, steel and interface properties the reader is referred to Rots [27].

The loading is applied to point A (Fig. 7) in the form of a concentrated load and the ensuing load-displacement diagram is given in Fig. 8. The present problem is well suited for demonstrating that straightforward application of a norm of incremental displacements to control the solution process often does not work effectively for localized failures. To this end we consider the incremental displacement fields just prior to and just beyond the limit point (Figs. 9 and 10). Prior to the limit point, the elastic deformations of the bar are relatively so great, that they dominate the norm of incremental displacements. Just beyond the peak, when the crack near the center-line has localized, the incremental deformations of the reinforcing bar nearly vanish (they even change sign, so that we again have a snap-back) and the concrete is the prime contributor to the total norm of incremental displacements. However, because of the relatively great magnitudes of the steel deformations just prior to the limit point, the arc-length in the displacement space is not influenced significantly. In this case, the degrees of
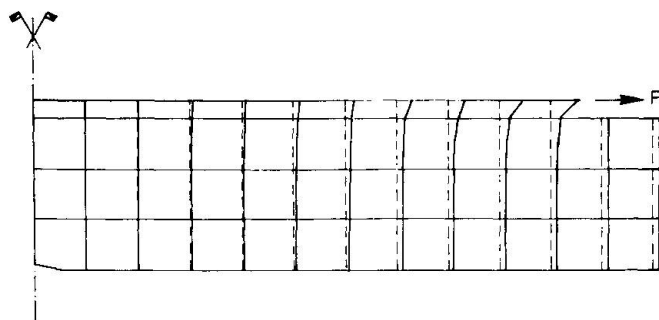
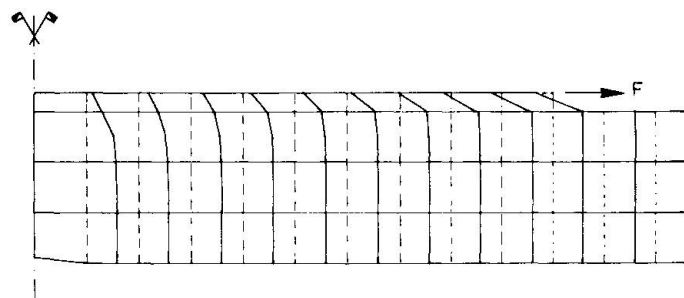Fig. 9. Incremental displacements just prior to the limit point.

Fig. 10. Incremental displacements just beyond the limit point.

freedom belonging to the steel have therefore been omitted from the norm of incremental displacements for overcoming the limit point. For traversing the valley in the load-displacement curve of Fig. 8 on the other hand, the solution process has been controlled by the displacements of the steel, as then these displacements increase monotonically.

The present example is also well suited for assessing the question whether an equilibrium state can be reached via a non-equilibrium path. It is the Author's experience that this is often possible when we adopt direct displacement control and if there exists another equilibrium state which is located "not too far away" from the current state. Indeed, when we attempted to analyze the present problem by prescribing the displacement of point A, we obtained a number of non-converged states just after the limit point. This non-equilibrium path is indicated by the dotted line in Fig. 8. However, after the crack had localized, we again obtained converged equilibrium states (dashed line in Fig. 8), which indicated that we had arrived on a new equilibrium path. This illustrates that reaching another part of the equilibrium path via a number of non-equilibrium states is sometimes possible, provided that there exists a new equilibrium state which is "sufficiently close" to the previous equilibrium state. Here, the tension-pull specimen contrasts with the example of Figs. 4 and 5, as in the latter case equilibrium could not be restored using direct displacement control.

6. STRAIN-SOFTENING AND SPURIOUS ZERO-ENERGY MODES

A major problem which presently hampers finite element calculations of material models in which use is made of strain-softening (like for instance crack models), is the fact that strain-softening triggers spurious zero-energy modes. This has been recognized by Dodds et al. [18], de Borst and Nauta [7] and Crisfield [17] for the case of underintegrated elements, but Rots and de Borst [29] have recently demonstrated that it may also happen for e.g., eight-noded elements with nine-point integration or four-noded elements with four-point integration. In fact, the analysis of the beam of Fig. 4 had to be terminated because of the occurrence of such a zero-energy mode which was triggered by strain-softening. A converged solution could no longer be obtained at the point where the load-displacement curve of Fig. 5 is terminated. An eigenvalue analysis of the tangent stiffness matrix revealed two negative eigenvalues. The eigenmode of Fig. 11 has a clear physical meaning, since it represents the localization which has by then progressed through the depth of the beam. The eigenmode of Fig. 12 is due to pathological behavior of one element at the top of the beam. It is emphasized that this behavior occurred in spite of the fact that nine-point Gaussian quadrature had been used. Later
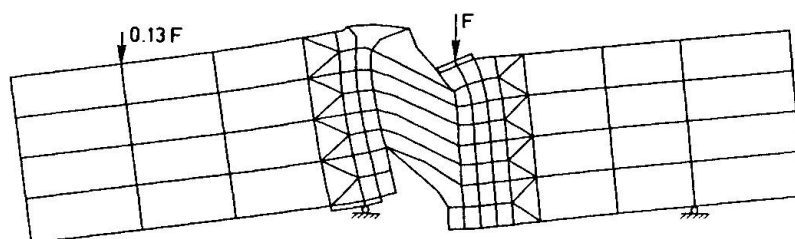
Fig. 11. First eigenmode at residual load of the unreinforced beam of Fig. 4.
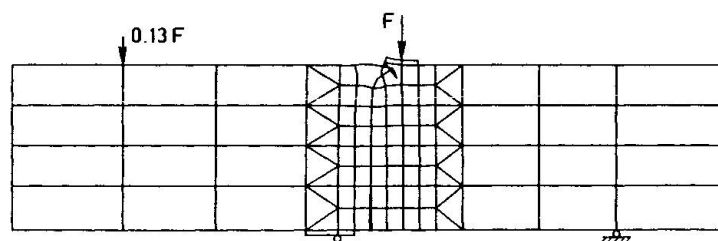

Fig. 12. Second eigenmode at residual load of the unreinforced beam of Fig. 4.

investigations also revealed that groups of four elements displayed spurious zero-energy modes when four-noded elements with four-point integration were employed [29].

7. CONCLUDING REMARKS

The essential features of the DIANA-crack model have been described. By dividing the total strain rate rigorously into a concrete and a crack strain rate, and by subdividing these strain rates again into a number of distinct contributions each of which is associated with a clearly defined physical phenomenon, it is possible to simultaneously analyze non-orthogonal cracks, creep, shrinkage, thermal dilatation and plasticity within a smeared context.

The incorporation of strain-softening models on integration point level may lead to unexpected behavior on structural level. An example is snap-back behavior. This phenomenon cannot be analyzed under direct displacement control, but only using indirect displacement control. Another consequence of deployment of strain-softening models is the possibility that bifurcations occur even under the assumption of small displacement gradients. Techniques have been discussed which permit tracing snap-back and post-bifurcation behavior. Some examples have been included to demonstrate that such techniques broaden the class of concrete structures which can be analyzed numerically.

On the other hand, it is not justified to state that any concrete structure can now easily be analyzed. A major problem which still hampers finite element analyses is the fact that strain-softening triggers the formation of spurious zero-energy modes. Techniques to control such modes in strain-softening materials must be developed before the limits of the class of problems which can be solved properly can be pushed further away.

Considering nonsymmetric stress-strain laws, we observe that little numerical work has been done. This is partly due to the fact that only a few finite element codes have been adapted for nonsymmetric solvers. But even if a finite element code with a nonsymmetric solver is available to the analyst, he faces the problem that the issues of stability and uniqueness of solution are much less clear-cut than for symmetric problems. This is particularly relevant when an analysis diverges, since in such a case it is much more difficult to trace whether the divergence is caused by failure or bifurcation phenomena in the model of the structure, or is simply caused by e.g., a trivial programming error. Yet, as soon as frictional processes take place, which is the case for concrete, stress-strain laws necessarily become nonsymmetric, which calls for an enhanced research effort to develop numerical procedures for such models.

ACKNOWLEDGEMENTS

REFERENCES

1. ARREA M. & INGRAFFEA A.R., Mixed-mode crack propagation in mortar and concrete. Report No. 81-13, Department of Structural Engineering, Cornell University, Ithaca, New York, 1981.
2. BARTON N., Deformation phenomena in jointed rock. Géotechnique 36, 1986, pp. 147-167.
3. BATHE K.-J., Finite element procedures in engineering analysis. Prentice-Hall, New Jersey, 1982.
4. BAZANT Z.P. & GAMBAROVA P., Rough cracks in reinforced concrete. ASCE J. Struct. Div. 106, 1980, pp. 819-842.
5. BAZANT Z.P. & OH B., Crack band theory for fracture of concrete. RILEM Materials and Structures 16, 1983, pp. 155-177.
6. BAZANT Z.P., BELYTSCHKO T. & CHANG T.-P., Continuum theory for strain softening. ASCE J. Eng. Mech. 110, 1984, pp. 1666-1692.
7. De BORST R. & NAUTA P., Non-orthogonal cracks in a smeared finite element model. Eng. Comput. 2, 1985, pp. 35-46.
8. De BORST R., Non-linear analysis of frictional materials. Dissertation, Delft University of Technology, Delft, 1986.
9. De BORST R., Numerical simulation of shear-band bifurcation in sand bodies. Numerical Models in Geomechanics (eds. G.N. Pande & W.F. van Impe), M. Jackson & Sons, Redrudth, 1986, pp. 91-98.
10. De BORST R., Computational aspects of smeared crack analysis. Computational Modelling of Reinforced Concrete Structures (eds. E. Hinton & D.R.J. Owen), Pineridge Press, Swansea, 1986, Ch. 2, pp. 44-83.
11. De BORST R. & Van Den BERG P., Analysis of creep and cracking in concrete members. Pre-prints RILEM Symp. on Creep and Shrinkage of Concrete: Mathematical Modeling (ed. Z.P. Bažant), Northwestern University, Evanston, Ill., 1986, pp. 527-538.
12. De BORST R., Computation of post-bifurcation and post-failure behavior of strain-softening solids. Comput. Struct. 25, 1987, pp. 211-224.
13. De BORST R., Smeared cracking, plasticity, creep and thermal loading - a unified approach. Comp. Meth. Appl. Mech. Eng., 1987.
14. De BORST R., Integration of plasticity equations for singular yield functions. Comput. Struct., 1987.
15. CRISFIELD M.A., A fast incremental/iterative procedure that handles snap-through. Comput. Struct. 13, 1981, pp. 55-62.
16. CRISFIELD M.A., Local instabilities in the non-linear analysis of reinforced concrete beams and slabs. Proc. Instn. Civ. Engrs. 73, 1982, pp. 135-145.
17. CRISFIELD M.A., Snap-through and snap-back response in concrete structures and the dangers of underintegration. Int. J. Num. Meth. Eng. 22, 1986, pp. 751-768.
18. DODDS R.H., DARWIN D., SMITH J.L. & LEIBENGOOD L.D., Grid size effects with smeared cracking in finite element analysis of reinforced concrete. SM Report No. 6, University of Kansas, Lawrence, Kansas, 1982.
19. DORR K., Kraft- und Dehnungsverlauf von in Betonzylindern zentrisch einbetonierten Bewehrungsstaben under Querdruck. Forschungsbericht No. 30, Institut für Massivbau der Technischen Hochschule Darmstadt, 1975.

20. HILL R., Some basic principles in the mechanics of solids without a natural time. J. Mech. Phys. Solids 7, 1959, pp. 209-225.

21. HILLERBORG A., MODEER M. & PETERSSON P.E., Analysis of crack formation and crack growth in concrete by means of fracture mechanics and finite elements. Cement and Concrete Research 6, 1976, pp. 773-782.

22. LITTON R.W., A contribution to the analysis of concrete structures under cyclic loading. Ph.D. Thesis, University of California, Berkeley, Calif., 1974,

23. RAMM E., Strategies for tracing the nonlinear response near limit points. Nonlinear Finite Element Analysis in Structural Mechanics, (Eds. W. Wunderlich, E. Stein & K.-J. Bathe), Springer Verlag, Berlin, 1981, pp. 63-83.

24. RIKS E., An incremental approach to the solution of snapping and buckling problems. Int. J. Solids Structures 15, 1979, pp. 529-551.

25. ROTS J.G., KUSTERS G.M.A. & BLAAUWENDRAAD J., The need for fracture mechanics options in finite element models for concrete structures. Proc. Int. Conf. Computer Aided Analysis and Design of Concrete Structures, Part 1, (eds. F. Damjanić et al.), Pineridge Press, Swansea, 1984, pp. 19-32.

26. ROTS J.G., NAUTA P., KUSTERS G.M.A. & BLAAUWENDRAAD J., Smeared crack approach and fracture localization in concrete. Heron 30, No. 1, 1985.

27. ROTS J.G., Bond-slip simulations using smeared cracks and/or interface elements. Research Report, Structural Mechanics Group, Department of Civil Engineering, Delft University of Technology, 1985.

28. ROTS J.G., Strain-softening analysis of concrete fracture specimens. Fracture Toughness and Fracture Energy of Concrete (Ed. F.H. Wittmann), Elsevier Science Publ., Amsterdam, 1986, pp. 137-148.

29. ROTS J.G. & De BORST R., Analysis of mixed-mode fracture in concrete. ASCE J. Eng. Mech., 1987.

30. ROTS J.G., HORDIJK D.A. & De BORST R., Numerical simulation of concrete fracture in 'direct' tension. Numerical Methods in Fracture Mechanics (eds. A.R. Luxmoore et al.), Pineridge Press, Swansea, 1987, pp. 457-471.

31. SCHREYER H.L. & CHEN Z., One-dimensional softening with localization. J. Appl. Mech., 1986, pp. 791-797.

32. WALRAVEN J.C. & REINHARDT H.W., Theory and experiments on the mechanical behavior of cracks in plain and reinforced concrete subjected to shear loading. Heron 26, No. 1A, 1981.

33. WILLAM K.J., Experimental and computational aspects of concrete fracture. Proc. Int. Conf. Computer Aided Analysis and Design of Concrete Structures, Part 1, (Eds. F. Damjanić et al.), Pineridge Press, Swansea, 1984, pp. 33-70.